Chapter 4

Wind Turbines Reactive Current Control During Unbalanced Voltage Dips

Ivan Jorge Gabe , Humberto Pinheiro and
Hilton Abílio Gründling

Additional information is available at the end of the chapter

http://dx.doi.org/10.5772/54095

1. Introduction

These chapter deals with the current references generation for the control of grid-connected voltage source converters, used in Wind Energy Generating Units (WEGU),operating under balanced and unbalanced voltage sags. The significant growing of power generation by wind turbines prompted grid operators to update the grid connection requirements. In the Early grid codes, WEGU disconnection were allowed during voltages dips and frequency disturbances. However, nowadays, they are required to stay connected during voltage dips resulted from faults at the grid side as well as support the grid voltage with additional reactive current [1-2]. Figure 1(a) shows a typical voltage supportability curve that a WEGU have to be able to meet during low voltage ride through (LVRT) operation, while Figure 1(b) shows the principle of voltage back up by reactive current support. Among the motivations for the system operators to put in place such requirements are (i) to minimize the loss of generation during grid faults mitigating in this way the mismatches between demand and generation and (ii) to improve the network voltage profile.

The voltage dips due grid faults are classified in seven different types [4], Figure 2 shows the phasorial representation of each possible voltage unbalance due grid faults. The type A voltage dip is results from balanced three-phase short-circuits. All the other six types result from unbalanced faults that give rise to the appearance of voltage negative sequence components. The later are caused by the phase-to-ground (type B), phase-to-phase (type E) and the two-phase-to-ground (type C) faults. On the other hand, types F, G and D arise due the propagation of unbalanced faults through Δ-Y transformers, as shown Figure 2 [5]. Note that the type G occurs only when a two-phase-to-ground faults propagates through two series connected Δ-Y transformers.

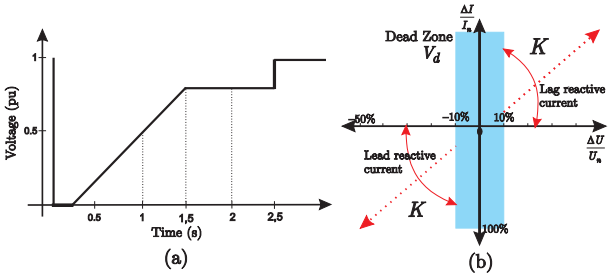

Figure 1. (a) LVRT curve, (b) Static characteristic for back up voltage operation [3].

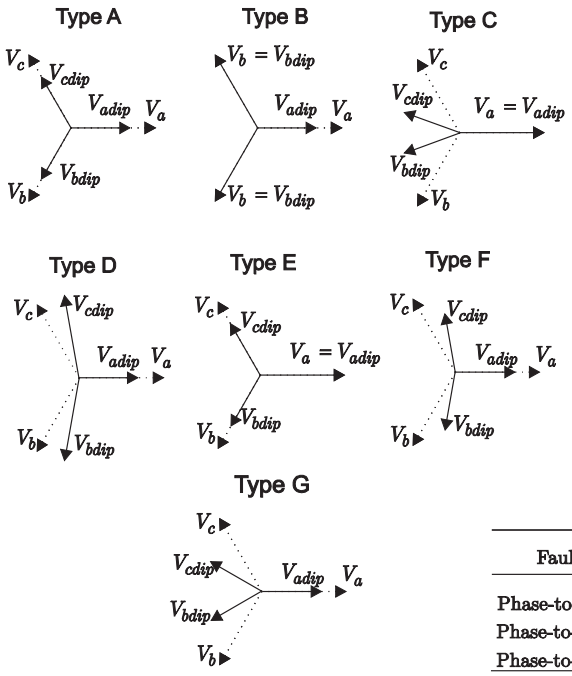

Propagation of Voltage dips Through a $\Delta - Y$ Connected Transformers

Fault	P_f	One $\Delta - Y$	Two $\Delta - Y$
Phase-to-Ground	B	C	D
Phase-to-Phase	E	D	C
Phase-to-Phase-to-Ground	C	F	G

Figure 2. Voltage Dips Classification.

A significant voltage deviation is defined as a voltage deviation with a magnitude greater than the voltage dead band V_d as shown in Figure 1(b). Nowadays, the great majority of the grid codes states that WEGU must stay connected and execute the voltage back up during three-phase balanced significant voltage deviations. However, grid faults give rise to unbalanced voltage sags in the most cases. So far, voltage support is not always a requirement. However, in recent grid codes [3], WEGU have to be capable to use at least 40% of their nominal current capacity to reactive current support during unbalanced voltage dips. The negative sequence

http://dx.doi.org/10.5772/54095

voltage brings some challenges for the WEGU operation, mainly concerning with the grid synchronization and the current control loop [6]. The grid synchronization has to be sufficiently fast and accurate to extract the negative and positive voltage sequences precisely, in order to generate the output current references. In [7] a synchronization method based on Kalman filter is presented for grid connected converters. This grid synchorization method has a good performance during balanced and unbalanced voltage dips. Another options are the traditional synchronous reference frame phase lock loop (PLL). In [8] are presented some variations on the traditional PLL for grid synchronization, making possible to extract the grid voltage sequence components even operating under unbalanced voltage conditions. On the other hand, the current controller has to be able to track negative sequence components. The conventional Synchronous Reference Frame Current Controller (SRFCC) ussualy presents a poor performance in these situations. The introduction of a double synchronous reference frame, synchronized with the positive and negative sequences, make possible to decouple the disturbance of the negative sequence on positive sequence current control loop and vice versa [9]. In [10] a current reference computation scheme was proposed in order to suppress the active power oscillations during unbalanced voltage sags as well as to avoid variations on the dc-link voltage. A review of current controller structures, in stationary and synchronous reference frames, is presented in [8]. Finally, if the current controller and the grid synchonization have a satisfactory performance, the impact of the WEGU on the grid directly dependents on how the current reference are defined. Many current reference methods for grid connected converters have been proposed aiming to reduce active and reactive power oscillations [11-12]. Nevertheless, emerging grid codes require voltage back up by reactive current injection during balanced and unbalanced voltage dips, where other issues, as the converter output current limitation for example, become more relevant than power oscillations supression. In addition, the injection of unbalanced currents during the LVRT operation may bring some useful effects as maximize the utilization of the converter current capacity and the reduction of the grid voltage unbalanced factor. However, depending on current reference methods, the effects may vary significantly [12].

In this chapter, a grid voltage negative sequence minimization (NSM) technique is proposed. It makes possible to inject unbalanced currents without exceeding the converter current ratings. To accomplish that, the proposed technique splits the current references in three parts. The first one is associated with the active power synchronized with the positive sequence voltage. The second one is related with the reactive power synchronized with the positive sequence while the third one is related with the reactive current synchronized with the negative sequence voltage. With the NSM technique, a simple and generic expression, depending only on the power references and voltages magnitudes information is derived to determine the possible amount of reactive power that can be added during an unbalanced voltage dip without overpass the converter current limits.

This chapter is organized as follow: Section II introduces some current reference methods used in the grid connected WEGU. Section III describes the proposed NSM method and the current limitation procedure. Section IV presents simulation results of the proposed method applied to a grid connected 2MW WEGU. Section V gives experimental results obtained in a grid

connected converter of 10kW under unbalance voltage dips. Finally, section VI summarizes the main topics covered in this chapter.

2. System description

A grid connected WEGU with synchronous generator and full power converter is shown in Figure 3. During an unbalanced voltage dip, positive and negative sequence voltages components appear on the grid side converter terminals. Let us consider the grid voltages vector defined as:

$$\mathbf{v} = \begin{bmatrix} v_a & v_b & v_c \end{bmatrix}, \tag{1}$$

where v_a, v_b and v_c are the WEGU grid side phase-to-ground voltages. On the same way, the converter output three-phase currents can be defined as:

$$\mathbf{i} = \begin{bmatrix} i_a & i_b & i_c \end{bmatrix}. \tag{2}$$

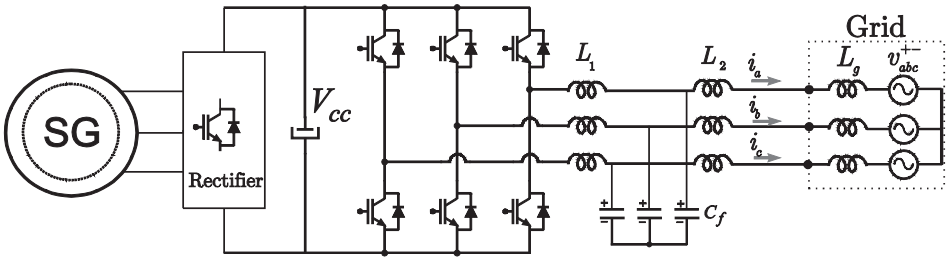

Figure 3. WEGU grid side converter.

In this chapter, the grid voltages and converter output currents are expressed in terms of their positive and negative sequence components at the fundamental frequency. In a three-phase three-wire system the voltages and currents vectors can be written as:

$$\mathbf{v} = \mathbf{v}^+ + \mathbf{v}^- \tag{3}$$

$$\mathbf{i} = \mathbf{i}^+ + \mathbf{i}^- \tag{4}$$

where the entries of $\mathbf{v}^+$ and $\mathbf{v}^-$ are the phase-to-ground sequence voltages. The $\mathbf{i}^+$ and $\mathbf{i}^-$ are composed by the output line positive and negative currents respectively. The instantaneous

http://dx.doi.org/10.5772/54095

active and reactive power can be obtained by the dot product and vector product of **v** and **i**, which results:

$$p = \mathbf{v}^{+}\mathbf{i}^{+} + \mathbf{v}^{+}\mathbf{i}^{-} + \mathbf{v}^{-}\mathbf{i}^{+} + \mathbf{v}^{-}\mathbf{i}^{-} \tag{5}$$

$$q = \mathbf{v}_{\perp}^{+}\mathbf{i}^{+} + \mathbf{v}_{\perp}^{+}\mathbf{i}^{-} + \mathbf{v}_{\perp}^{-}\mathbf{i}^{+} + \mathbf{v}_{\perp}^{-}\mathbf{i}^{-} \tag{6}$$

where $\mathbf{v}_{\perp}$ is the voltage vector composed by the 90° lagged voltages in relation to the phase-to-ground voltages of vector **v**.

A classical solution of the reactive current support during unbalanced voltage dips is the injection of only positive sequence currents, following the same strategy used in balanced voltage dips [14]. This procedure may produce undesirable overvoltages on the non-affected phase and increase the unbalance factor between the grid voltages. On the other hand, during unbalanced voltage dips, it is possible to use the additional converter current capacity to mitigate the voltage unbalance. During the LVRT operation, the unbalanced output currents have to be controlled accurately, in order to avoid the converter to trip. On the next section, some basic selected current reference generation strategies are summarized to introduce the proposed negative sequence minimization reference current technique.

2.1. Literature review

A review of the main strategies that synthesizes with simplicity the current reference methods for grid connected converters during unbalanced voltage dips [8] [12] are presented in the following.

2.1.1. Instantaneous Active Reactive Control (IARC)

The most intuitive way to compute the current references during voltage dips is using the vector of voltages **v** and $\mathbf{v}_{\perp}$ and the active and reactive power references P^{*} and Q^{*}. The current reference vector can be obtained as:

$$\mathbf{i}_{p}^{*} = \frac{P^{*}}{|\mathbf{v}|^{2}}\mathbf{v} \tag{7}$$

$$\mathbf{i}_{q}^{*} = \frac{Q^{*}}{|\mathbf{v}|^{2}}\mathbf{v}_{\perp} \tag{8}$$

$$\mathbf{i}^{*} = \mathbf{i}_{p}^{*} + \mathbf{i}_{q}^{*} \tag{9}$$

The reference current vector $\mathbf{i}^*$ is composed by the sum of the active power current vector $\mathbf{i}_p^*$, where the components are in phase with the voltages on $\mathbf{v}$, and the reactive power current $\mathbf{i}_q^*$, where the components are in phase with $\mathbf{v}_\perp$.

In the case of balanced phase voltages, $\mathbf{v}^-=0$ and as a result the norm of the vector $|\mathbf{v}|$ is a constant value leading to sinusoidal balanced output currents. However, if some unbalance is present, $|\mathbf{v}|$ has an oscillation on twice de fundamental frequency. As a consequence, the current references will have and undesired harmonic components. Figure 4 (a) shows the resulting current references during a type B voltage dip at the terminals of a 1MW WEGU. Note that the active power is reduced during the fault, to allow the reactive current support. Before and after the voltage dip, only active power is delivered to the grid. It is possible to note that the active and reactive power are kept constant at the price of introducing harmonics on the output currents.

2.1.2. Balanced Positive Sequence (BPS)

In order to get only sinusoidal and balanced currents on the converter output, the current references are synchronized with the positive sequence voltage vector $\mathbf{v}^+$.

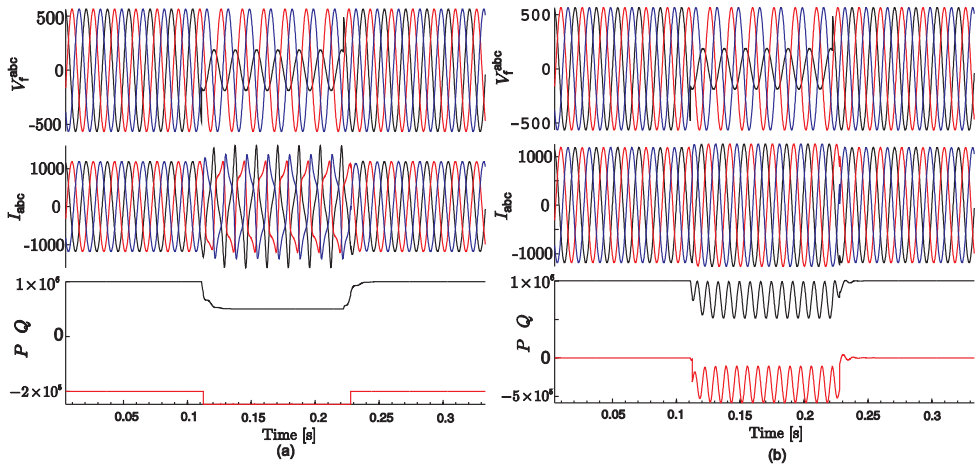

Figure 4. Reference currents and output power obtained during a type B unbalanced voltage dip to a a line voltage of 690Vrms, (a) references currents obtained using IARC and resulting output powers, (b) references currents obtained using BPS and resulting output powers.

The $\mathbf{i}_p^*$ and $\mathbf{i}_q^*$ reference currents are given by:

http://dx.doi.org/10.5772/54095

$$\mathbf{i}_p^* = \frac{P^*}{\left|\mathbf{v}^+\right|^2}\mathbf{v}^+ \tag{10}$$

$$\mathbf{i}_q^* = \frac{Q^*}{\left|\mathbf{v}^+\right|^2}\mathbf{v}_\perp^+ \tag{11}$$

Figure 4(b) shows the BPS reference currents obtained during type B voltage dip. The currents are always balanced even during the unbalanced voltage dips. The output powers are oscillatory due the interaction of the negative sequence voltage and the positive sequence currents.

2.1.3. Positive and Negative Sequence Control (PNSC)

This strategy allows the control of the positive and negative sequence currents associated with the active and reactive powers. The $\mathbf{i}_p^*$ and $\mathbf{i}_q^*$ vectors are obtained as follows:

$$\mathbf{i}_p^* = \frac{P^*}{\left|\mathbf{v}^+\right|^2 - \left|\mathbf{v}^-\right|^2}(\mathbf{v}^+ - \mathbf{v}^-) \tag{12}$$

$$\mathbf{i}_q^* = \frac{Q^*}{\left|\mathbf{v}^+\right|^2 - \left|\mathbf{v}^-\right|^2}(\mathbf{v}_\perp^+ - \mathbf{v}_\perp^-) \tag{13}$$

Figure 5 shows the PNSC resulting currents during a type B voltage dip. This strategy allows combine a set of positive and negative sequence voltages with the objective of cancelling the active power oscillations.

As seen, there are many possibilities to define the reference current. The injection of distorted currents in the IARC is undesired since generation units usually have to avoid the injection of harmonic content into the grid, even during the LVRT operation due the power quality issue. The BPS method overcomes current distortion issue since it injects only balanced currents to the voltage back-up. As a consequence, it allows boosting the grid positive sequence voltage if required. On the other side, the PNSC strategy shows the possibility to combine the negative sequence components to eliminate output power oscillations, resulting in unbalanced output currents. However, the important point of the mitigation of negative sequence voltage is not addressed. The next section presents the NSM technique, where the positive and negative sequence voltages are used to inject reactive current during the LVRT operation.

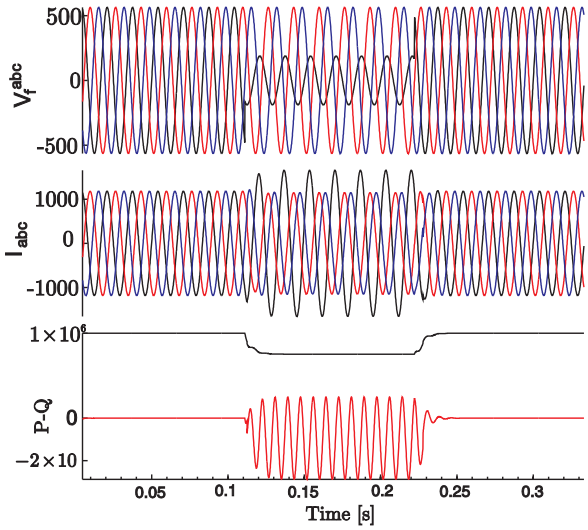

Figure 5. Reference currents and output active and reactive powers during a type B voltage dip. Gains k_p=1 and k_q=1 for balanced currents and k_p=1 and k_q=0.5 for unbalanced currents.

3. Negative Sequence Voltages Minimization (NSM) technic

During the LVRT operation, the reactive power reference Q^* is obtained as shown in equation (15), where I_q follows the reative current support rules stated in [3]

$$I_q = \frac{K(V^+ - \overline{V}_1^+) - V_d}{V_n} I_n. \tag{14}$$

Gain K is adjustable from 1 to 10, depending on an agrimment with the grid utility operator, V^+ is the positive sequence voltage immediatly after the voltage dip occurs, $\overline{V}_1^+$ is the 1-minute average value of the positive sequence voltage prior to the voltage dip, V_n is rated line-to-line Root-Mean-Square RMS voltage, V_d is the voltage deadband and I_n is the rated RMS line current of the WEGU.

As a result, the reactive power reference Q^* during the LVRT operation can be expressed as:

$$Q^* = 3V^+ I_q \tag{15}$$

http://dx.doi.org/10.5772/54095

According to the German grid code [3], in three-phase voltage dips, the WEGU has to be able to use up to 100% of its current rating capacity to the voltage support, accordingly with Figure 1(b). During a significant voltage deviation, the current associated with the active power, has to be reduced in the benefit of the reactive current feed-in. In the case of unbalanced voltage dips, the significant voltage deviation is detected if the $V^{+}<0.9V_{n}$, in this case the WEGU must be technically able to feed in a reactive current of at least 40% of the rated current. In [14], a WEGU operation mode during significant voltage deviations is demonstrate, the current injected are balanced and in phase with the positive sequence voltages only.

On the unbalanced voltage dips case, 40% of the current capacity has to be used during the reactive current support. There is no obligation to use the remaining current capacity. In addition, it is well know that the utilization factor of a typically WEGU range from 20% to 40% [15]. A good alternative in these cases is injecting reactive current synchronized with the negative sequence in order to mitigate unbalance between the voltages.

As a consequence, the active and reactive current references, to normal operation and during voltage dips can be defined as

$$\mathbf{i}_{p}^{*}=\frac{P^{*}}{\left|\mathbf{v}^{+}\right|^{2}}\mathbf{v}^{+} \tag{16}$$

$$\mathbf{i}_{q}^{*}=\frac{Q^{*}}{\left|\mathbf{v}^{+}\right|^{2}}\mathbf{v}_{\perp}^{+}+\frac{B^{*}}{\left|\mathbf{v}^{-}\right|^{2}}\mathbf{v}_{\perp}^{-} \tag{17}$$

where B^{*} is the negative sequence reactive power reference. Note that in equation (16), the negative sequence voltage is not included. The problem that arises is how to find B^{*} in order to guarantee that the output current do not overpass a pre-defined limit. In the next subsection, a current limitation algorithm is derived.

3.1. Current limitation

Let us assume that the output limit current of a grid-connected converter is the same in each phase. The current amplitude range in each phase can be defined in the interval $i_{x}=\left[-I_{x}^{\lim},\quad I_{x}^{\lim}\right]$, where $x=a,\ b,\ c$. In addition, as a three wire converter is considered, the sum of all the three output currents is always zero. Considering this conditon, is possible to define a set of possible output currents and gathering them into a vector $\mathbf{i}_{abc}$.

To obtaine the currents in the $\alpha\beta$ reference frame, the well-known abc-$\alpha\beta$ transformation is applied to the all the possible $\mathbf{i}_{abc}$ vector.

$$\mathbf{i}_{\alpha\beta} = \sqrt{\frac{2}{3}} \begin{bmatrix} 1 & -\frac{1}{2} & -\frac{1}{2} \\ 0 & \frac{\sqrt{3}}{2} & -\frac{\sqrt{3}}{2} \\ \frac{1}{\sqrt{2}} & \frac{1}{\sqrt{2}} & \frac{1}{\sqrt{2}} \end{bmatrix} \mathbf{i}_{abc}. \tag{18}$$

where $\mathbf{i}_{\alpha\beta}$ is the current vector in the $\alpha\beta$ reference frame.

The mapping of all possible $\mathbf{i}_{abc}$ vectors in the $\alpha\beta$ reference frame are confined within a hexagon, as show in Figure 6. Hence, to guarantee that the output currents are limiting in the abc-framework, is necessary to limit the $\alpha\beta$ reference currents inside the hexagon. In a normal operation situation, i_α and i_β are balanced and sinusoidal, consequently the $\mathbf{i}_{\alpha\beta}$ vector describes a circle inside the hexagon.

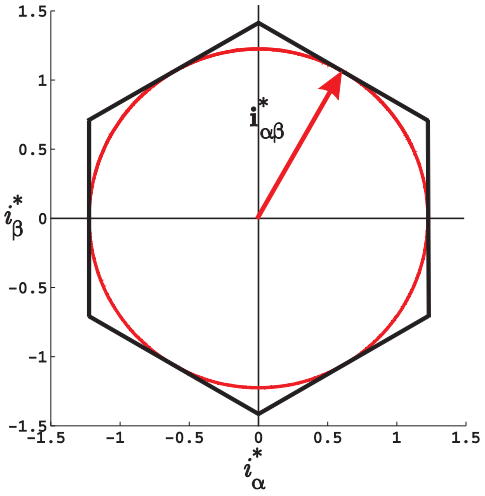

Figure 6. (a) Converter current capability curve in $\alpha\beta$ coordinates.

To develop a methodology to compute B^*, and assures that the output currents stay inside the hexagon, it is necessary to analyze the behavior of the output currents obtained by equations (16) and (17). Assuming that the phase voltages on vector **v** in (1) can be expressed as:

$$\begin{aligned} v_a &= v_a^+ + v_a^- \\ v_b &= v_b^+ + v_b^- \\ v_c &= v_c^+ + v_c^- \end{aligned} \tag{19}$$

http://dx.doi.org/10.5772/54095

where δ_v is the voltage angle and V_{abc} are the phase magnitudes.

The synchronization system presented in [7] filters the fundamental frequencies of the phase voltages of (19). In addition, the 90° lagged components of each phase voltage are also available. Applying the transformation in [16], the positive and negative sequence voltages can be expressed as:

$$v_a^+ = V^+ \sin(\omega t + \delta_v^+) \tag{20}$$

$$v_b^+ = V^+ \sin(\omega t + \delta_v^+ - 120^\circ) \tag{21}$$

$$v_b^+ = V^+ \sin(\omega t + \delta_v^+ + 120^\circ) \tag{22}$$

$$v_a^- = V^- \sin(\omega t + \delta_v^-) \tag{23}$$

$$v_b^- = V^- \sin(\omega t + \delta_v^- + 120^\circ) \tag{24}$$

$$v_b^- = V^- \sin(\omega t + \delta_v^- - 120^\circ) \tag{25}$$

The 90° lagged components of each phase voltage are also available:

$$v_{aq}^+ = V^+ \sin(\omega t + \delta_v^+ + 90^\circ) \tag{26}$$

$$v_{bq}^+ = V^+ \sin(\omega t + \delta_v^+ - 30^\circ) \tag{27}$$

$$v_{cq}^+ = V^+ \sin(\omega t + \delta_v^+ + 210^\circ) \tag{28}$$

$$v_{aq}^- = V^- \sin(\omega t + \delta_v^- - 90^\circ) \tag{29}$$

$$v_{bq}^- = V^- \sin(\omega t + \delta_v^- + 30^\circ) \tag{30}$$

$$v_{cq}^{-} = V^{-}\sin(\omega t + \delta_{v}^{-} - 210^{\circ}) \tag{31}$$

where δ_v^+ and δ_v^- are the positive and negative reference angles in relation to δ_v. Using the abc-$\alpha\beta$ transformation to get the voltages of (19) in the $\alpha\beta$f ramework, we obtain

$$\begin{bmatrix} v_{\alpha} \\ v_{\beta} \end{bmatrix} = T_{\alpha\beta} \begin{bmatrix} v_{a} \\ v_{b} \\ v_{c} \end{bmatrix}. \tag{32}$$

The same procedure can be applied to (20-31), resulting in the following variables respectively v_{α}^{+}, v_{β}^{+}, v_{α}^{-}, v_{β}^{-}, $v_{\alpha\perp}^{+}$, $v_{\beta\perp}^{+}$, $v_{\alpha\perp}^{-}$ and $v_{\beta\perp}^{-}$.

The reference currents in the $\alpha\beta$ framework, accordingly with the equations (16) and (17) can be expressed as

$$i_{\alpha}^{*} = i_{\alpha p}^{+} + i_{\alpha q}^{+} + i_{\alpha q}^{-} \tag{33}$$

$$i_{\beta}^{*} = i_{\beta p}^{+} + i_{\beta q}^{+} + i_{\beta q}^{-} \tag{34}$$

where the positive sequence currents are determined by

$$i_{\alpha p}^{+} = \frac{P^{*}}{\left|\mathbf{v}^{+}\right|} v_{\alpha}^{+} \tag{35}$$

$$i_{\beta p}^{+} = \frac{P^{*}}{\left|\mathbf{v}^{+}\right|} v_{\beta}^{+} \tag{36}$$

$$i_{\alpha q}^{+} = \frac{Q^{*}}{\left|\mathbf{v}^{+}\right|} v_{\alpha\perp}^{+} \tag{37}$$

$$i_{\beta q}^{+} = \frac{Q^{*}}{\left|\mathbf{v}^{+}\right|} v_{\beta\perp}^{+}. \tag{38}$$

http://dx.doi.org/10.5772/54095

The negative sequence voltages are given by:

$$i_{\alpha q}^{-} = \frac{B^{*}}{\left|\mathbf{v}^{-}\right|} v_{\alpha\perp}^{-} \tag{39}$$

$$i_{\beta q}^{-} = \frac{B^{*}}{\left|\mathbf{v}^{-}\right|} v_{\beta\perp}^{-}. \tag{40}$$

In the balanced case, the reference currents are in phase with the positive sequence voltage. In the case of $P^{*}>0$, $Q^{*}\neq 0$ and $B^{*}=0$, the representation of the current vector $\mathbf{i}^{*}_{\alpha\beta}$ is a circle. On the other hand, if B^{*} is not null, reactive power currents synchronized with the negative sequence voltage are added in the reference currents of equation (33-34). As a consequence, the graphically representation of the reference currents describes an ellipse on the $\alpha\beta$ plane. Figure 7 shows the current limit circle and an inscribed ellipse. It is important to observe that i_{α} and i_{β} currents do not reach its maximum possible values, but the $|\mathbf{i}^{*}_{\alpha\beta}|$ reaches the circle in some point, producing the maximum allowed output current on the abc-framework.

Taking equations (35-40), is possible to define the constants k_2, k_3 and k_1:

$$k_1 = \frac{P^{*}}{\left|\mathbf{v}^{+}\right|} \tag{41}$$

$$k_2 = \frac{Q^{*}}{\left|\mathbf{v}^{+}\right|} \tag{42}$$

$$k_3 = \frac{B^{*}}{\left|\mathbf{v}^{-}\right|} \tag{43}$$

Replacing equations (41-43) in (33-34) and writing the $\alpha\beta$ references components in sine and cosine, the current references can be expressed as:

$$i_{\alpha}^{*} = k_1 \sin(\omega t + \delta_{v}^{+}) - k_2 \cos(\omega t + \delta_{v}^{+}) - k_3 \sin(\omega t + \delta_{v}^{-}) \tag{44}$$

$$i_{\beta}^{*} = k_1 \cos(\omega t + \delta_{v}^{+}) + k_2 \sin(\omega t + \delta_{v}^{+}) + k_3 \cos(\omega t + \delta_{v}^{-}) \tag{45}$$

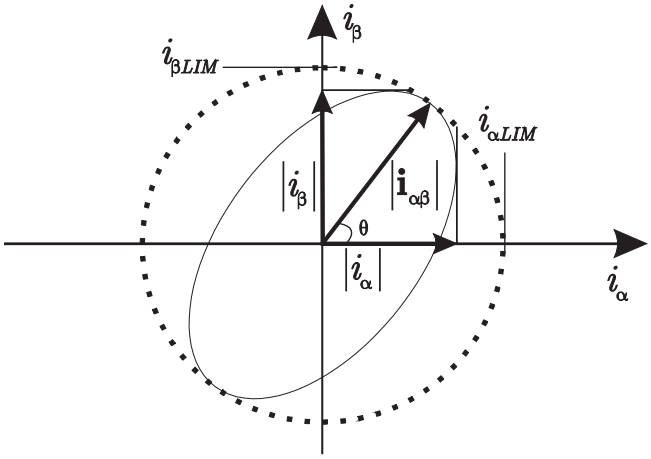

Figure 7. Negative sequence component effect on the norm of currents vector $|\mathbf{i}_{\alpha\beta}|$.

The challenge is to find an expression that defines the norm of a given set of current references i_α^* and i_β^*. Making $\omega t + \delta_v^+ = \theta$ and $\omega t + \delta_v^- = \theta + \theta\_$ on equations (44) and (45) results

$$i_\alpha^* = k_1 \cos(\theta) + k_2 \sin(\theta) + k_3 \cos(\theta + \theta\_) \tag{46}$$

$$i_\beta^* = k_1 \sin(\theta) - k_2 \cos(\theta) - k_3 \sin(\theta + \theta\_) \tag{47}$$

In order to find the norm of vector $\mathbf{i}_{\alpha\beta}^*$, considering the current references expressed in (46-47), is possible to write that

$$\left\|\mathbf{i}_{\alpha\beta}^*\right\| = \sqrt{(k_1 \sin(\theta) - k_2 \cos(\theta) - k_3 \sin(\theta + \theta\_))^2 + (k_1 \cos(\theta) + k_2 \sin(\theta) + k_3 \cos(\theta + \theta\_))^2}. \tag{48}$$

Taking the derivative in function of θ and equal to zero, is possible to find a point of maximum of the ellipse:

http://dx.doi.org/10.5772/54095

$$\frac{d}{d\theta}\sqrt{(k_1\sin(\theta)-k_2\cos(\theta)-k_3\sin(\theta+\theta\_))^2+(k_1\cos(\theta)+k_2\sin(\theta)+k_3\cos(\theta+\theta\_))^2}=0 \tag{49}$$

Simplifying the result of equation (49), results in:

$$4k_2k_3\cos(2\theta+\theta\_)-4k_1k_3\sin(2\theta+\theta\_)=0. \tag{50}$$

Solving equation (50) in terms to θ:

$$\theta=\frac{\tan^{-1}\left(\frac{k_2}{k_1}\right)-\theta\_}{2} \tag{51}$$

Substituting (51) in (48) results an expression that determines the norm of $\mathbf{i}^*_{\alpha\beta}$ in function of the k_1, k_2 and k_3 parameters:

$$\left\|\mathbf{i}^*_{\alpha\beta}\right\|=\sqrt{k_1^2+k_2^2+k_3^2+2k_3\sqrt{k_1^2+k_2^2}}. \tag{52}$$

An important result of (52) is the possibility to get the maximum norm without taking use of the angles δ_v^+ and δ_v^-. Making $\|\mathbf{i}^*_{\alpha\beta}\|= I^{\lim}_{\alpha\beta}$ is possible to solve equation (52) to k_3. The resulting equation gives us two possible solutions

$$k_3^{+-}=\frac{-2k_1^2-2k_2^2\pm 2I^{\lim}_{\alpha\beta}\sqrt{k_1^2+k_2^2}}{2\sqrt{k_1^2+k_2^2}}. \tag{53}$$

Only the positive solution for equation (53) is valid, once that $k_3\geq 0$ for the reactive capacitive power injection. So, B^* can is given by

$$B^*=k_3^+\left|\mathbf{v}^-\right|. \tag{54}$$

Figure 8(a) shows the $\|\mathbf{i}^*_{\alpha\beta}\|$ trajectory in the $\alpha\beta$ plane for k_3=0. Otherwise, in Figure 8 (b), (c) and (d), presents the resulting ellipse and the circle with the norm obtained by equation (52). The maximum norm is finding accurately, independent on the voltage phase angles. The angle θ depends on the active and reactive power references and on the negative sequence angle δ_v^-, as shown in equation (51).

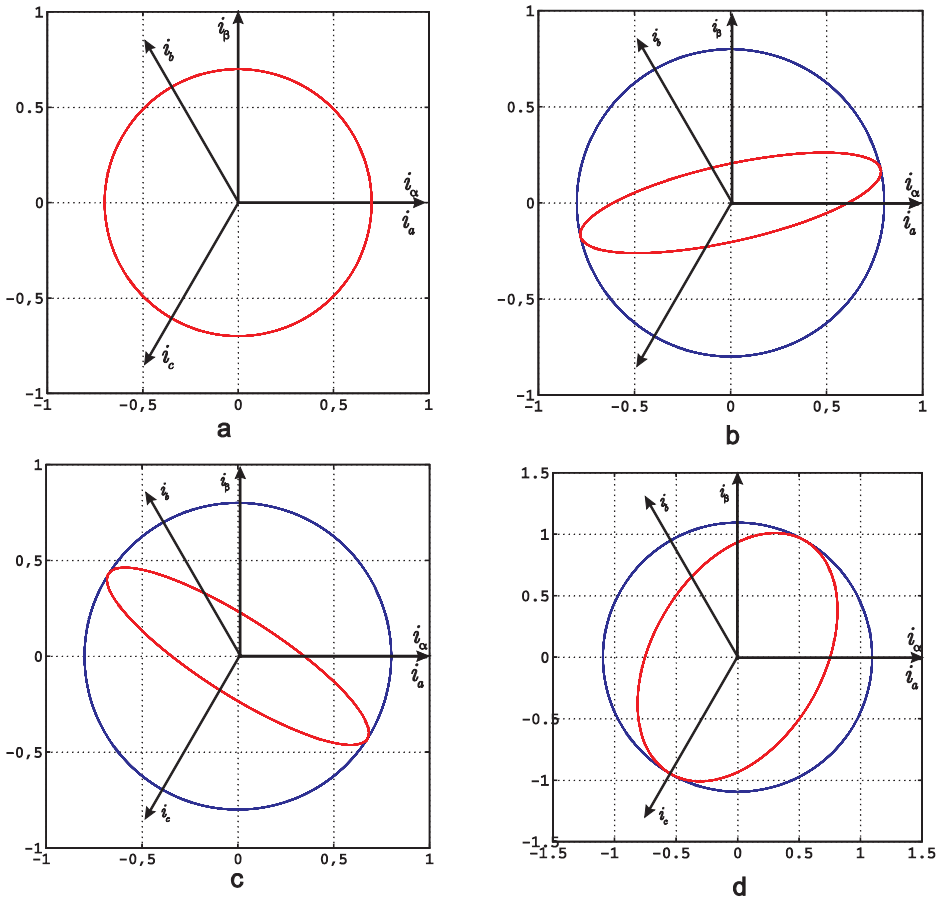

Figure 8. (a) $\alpha\beta$ framework current norm for $k_1=0.7I_n$, $k_2=0$ e $k_3=0$, (b) Circle with radius computed by (42) and resulting ellipse for $k_1=0$, $k_2=-0.5I_n$, $k_3=0.3I_n$ $\boldsymbol{\theta}$=40°, (c) Circle and ellipse for $k_1=0$, $k_2=0.5I_n$, $k_3=0.3I_n$e $\boldsymbol{\theta}$=40°, (d) Circle and ellipse for $k_1=0.6I_n$, $k_2=0.5I_n$, $k_3=0.3I_n$e $\boldsymbol{\theta}$=40°.

4. Simulation results

In order to demonstrate the NSM current limitation algorithm, a WEGU system composed by a three phase, three wire converter, is connected to the electrial network show in Figure 9. The WEGU is connected on the low voltage side of the Transformer T3 on a line to line voltage of 690 Vrms and with a nominal power of $P_n=2MW$. The short circuit ratio on the PCC is near to 4, what represent a weak grid model. The voltage source converter male use of a synchronization system base on Kalman Filter, as presented in [7]. The current controllers are implemented in stationary frames and are based in resonant controllers as presented in [17]. All the

http://dx.doi.org/10.5772/54095

simulations are executed in Matlab/Simulink ®. To demonstrate the NSM algorithm performance a two-phase-to-ground fault on the point (P1) in the distribution feeder will be tested. Figure 10 shows the resulting variables. Prior the fault, $t < T_1$, the WEGU is injecting $0.2P_n$ into the grid. At T_1 the fault occurs, and the WEGU LVRT operation initiate. In order to meet the grid code requirements [3], 40% of the current converter capacity is used to inject balanced reactive currents using the BPS strategy.

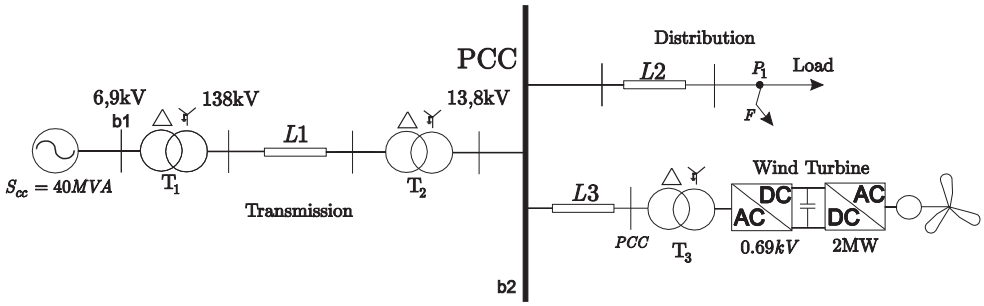

Figure 9. Electrical network for the evaluation of the NSM model.

On Fig. 10(c) is possible to see how the current support boost the positive sequence voltage from 388V to 497V at the PCC. However, the negative sequence almost remaing the same, changing from 161V to 165V. At time T_2, the current reference strategy is switched to the NSM. Equation (53) computes the value of k_3 in order to the pre-defined $I_{\alpha\beta}^{\lim}$. Is possible to see that output current i_a reach the maximum allowed current, in this case setted to 2366 A. The positive sequence voltage remains the same as in $t < T_2$, but the negative sequence voltage reduces from 165V to 67V. The unbalanced factor on the PCC voltages of Figure 10(b) is clearly lower. One of the more relevant result of this work can be infered on Figure 10(d). The magnitude of the current reference vector $\mathbf{i}^*_{\alpha\beta}$ is computed by equation (52) during all the simulation. It can be seen that the result is valid to balanced and unbalanced currents. Between times T_2 and T_3, the currents are unbalanced and the value of $\|\mathbf{i}^*_{\alpha\beta}\|$ does not reach the current references peak value as in the balanced case. Figure 11 depictes the graphically trajectory of $\mathbf{i}^*_{\alpha\beta}$ during the balanced (BPS) and unbalanced (NSM) operation. The ellipse trajectory does not overpass the current limit circle what guarantees the current limitation on the abc framework. In addition, is worth to point out that i^*_α and i^*_β will reach its maximum values only if the resulting ellipse is aligned with the α or β axis. At T_3 the fault is cleared and the reactive current support is finished, the active power reference stays in $0.2P_n$ during all the simulation time.

An important parameter to measure the level of unbalance voltages is the unbalanced factor [13] given by:

$$\%VUF = \frac{\left|v^{-}\right|}{\left|v^{+}\right|} \times 100 \tag{55}$$

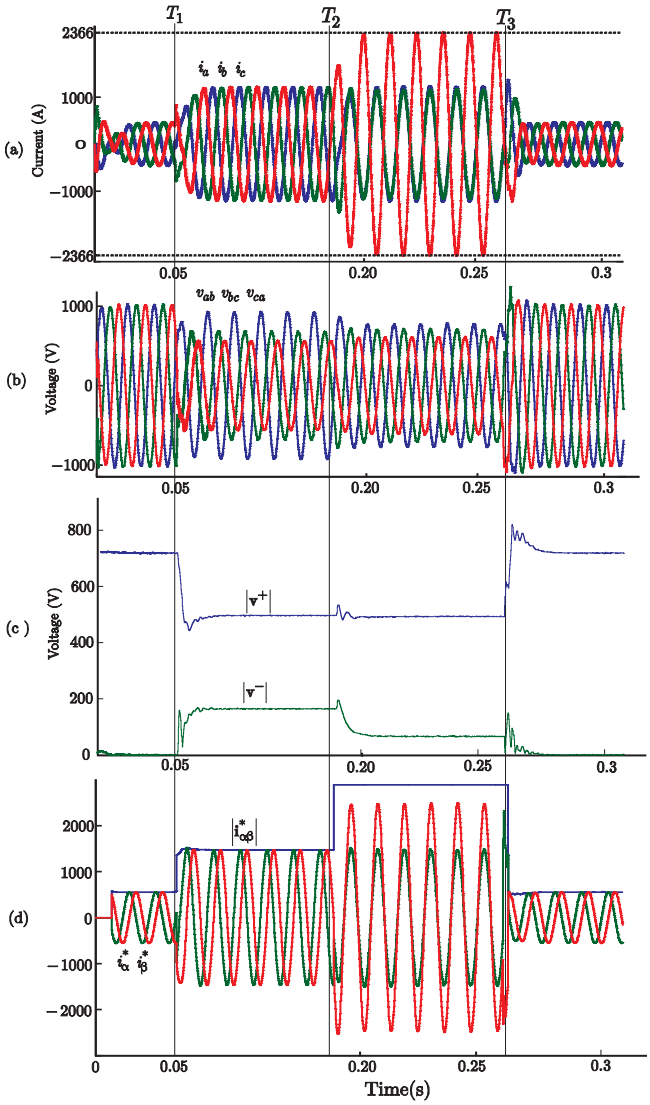

Figure 10. BPS and NSM strategies during an unbalanced voltage dip on weak grid conditions: (a) Grid connected converter output currents, (b) PCC voltages. (c) Positive and negative sequence voltages magnitude, (d) Reference currents and $\mathbf{i}^*_{\alpha\beta}$ computed by equation (52).

http://dx.doi.org/10.5772/54095

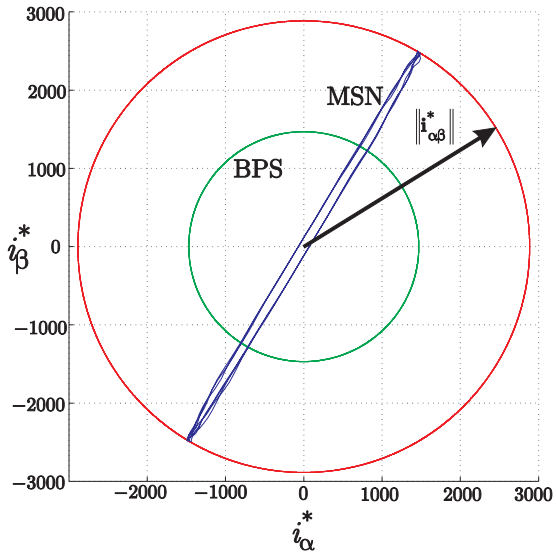

Figure 11. Reference current trajectory in the current spaces.

In order to compare the performance of the current reference strategies, a set of simulations to evaluate the unbalance factor are investigated. Two diferrent faults on the distribuiton feeder (P1) are considered. Fault F1 is a phase-to-ground fault that results in a type C voltage dip on the converter terminals. Fault F2 is a phase-to-phase to ground fault, as a consequence a type F voltage dip arise on the WEGU terminals. Another two issues are important to be considered. The active power level on the moment of the fault and the short circuit ratio on the PCC. To F1 and F2, two levels of active power are considered: $0.2P_n$ and $0.5P_n$. Above this active power level, and taking into account that 40% of the reactive current support is done by balanced currents, there will be no much remaing current capacity available to inject negative sequence reactive current. In addition, the transmisison line L1 and distribution line L3 have their lenghts reduced in order do modify the short circuit ratio on the PCC to 10. In all this simulations, the back up voltage support rulles of [3] are followed. Table 1 shows the resulting unbalance factor for the simulations using BPS, NSM or PNSC current reference strategies. By the analysis of the simulations results, some conclusions can be inferred:

- The BPS has a poor performance in all situation, when compared with the PNSC and NSM strategies;
- The type of faults does not change the effectiveness of the strategies;
- On the $0.5P_n$ active power level, the PNSC and NSM have similar performances in the strong and weak grid conditions;
- The NSM has a better performance in the $0.2P_n$ active power level, specialy in the weak grid condition.

In the next section, some experimental results of the NSM strategy are presented

Type of Fault	Phase-to-Ground (F1)				Phase-to-Phase to Ground (F2)			
Short Circuit Ratio	4		10		4		10	
Strategies\Active Power	0.2Pn	0.5Pn	0.2Pn	0.5Pn	0.2Pn	0.5Pn	0.2Pn	0.5Pn
PNSC	19,4%	18,3%	19,5%	19,4%	22,7%	20,2%	25,6%	29,8%
BPS	25%	23,5%	24,4%	23,1%	33,2%	30,6%	34,8%	33,8%
MSN	9,9%	18,6%	11,4%	16%	13,2%	23,3%	23,6%	29,6%

Table 1. Resulting unbalanced Factors.

5. Experimental results

The experimental setup is composed by a three-phase PWM voltage-source converter inveter of 10-kVA, and an impedance switching voltage sag generator (VSG) connected to the grid as shown in Fig. 12. The synchornization system extract the sequence components by filtering the grid phase voltages. Equation (15) gives the positive sequence reactive power reference Q^* and equation (40) gives the negative sequence power reference B^*. The switching frequency is f_s=10kHz, inductors $L_1 + L_2$=2mH, C_f =40μF, V_{dc}=200V and line to line voltage of 100 V_{rms}.

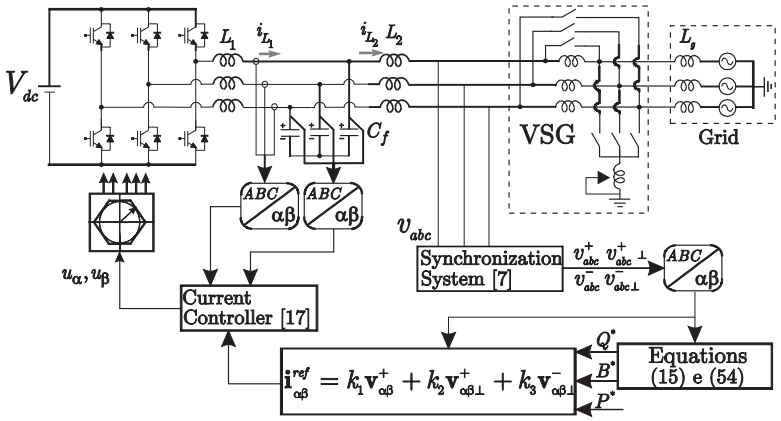

Figure 12. Experimental setup.

Considering the grid connected inverter injecting 500W into the grid prior the fault. The VSG is set to perform a phase-to-phase-to ground fault, with duration of 500ms, resulting in a type C voltage dip. The impedances are set to provide a reduction on the positive sequence voltage

http://dx.doi.org/10.5772/54095

of 35%. Figure 13 (a) shows the resulting line-to-line voltages on the on the converter terminals with a peak value of 152V. The positive sequence voltage decrease to 121V during the fault and the negative sequence voltage arise to 27V. Figure 13(b) shows the converter output currents and the power references before, during and after the voltage dip. Before the fault, the converter is only injecting active power into the grid. As the unbalanced voltage dip initiate, the NSM strategy compute the reactive power references by equations (15) and (54). The current limit is set to 20 A, i_a current reachs this limit as shows the red line limit.

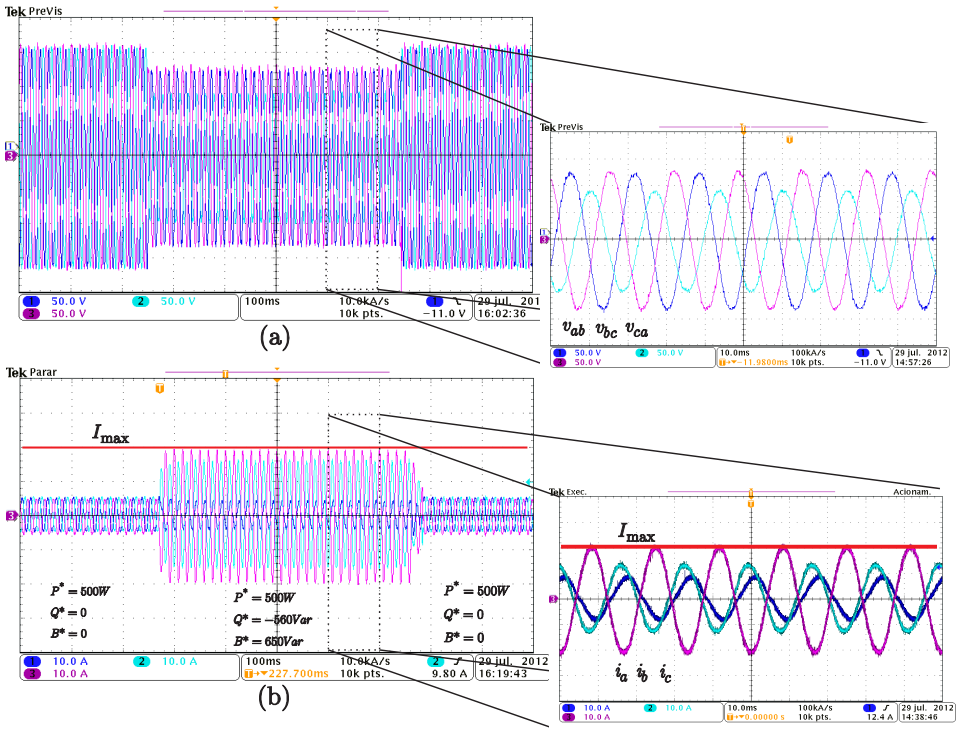

Figure 13. Experimental results, (a) line to line voltages on the PCC, (b) output currents.

6. Conclusions

This chapter has presented a new control method to limit the output current grid connected converter during unbalanced voltages sags voltage sags. WEGU are required to contribute for the voltage back up after balanced and unbalanced voltage dips. However, during unbalanced voltage dips negative sequence voltages arise on the wind turbine terminals. The voltage support by reactive current support is required, and the WEGU has to use at least 40% of their current capacity to back up the grid voltage. The injection of positive sequence reactive current

during faults permits boosting the voltage at the PCC. In addition, the injection of negative sequence reactive power allows reduce the unbalance between the voltages. Hence, if unbalanced currents may be injected into the grid, to assure that the converter do not disconnect during the LVRT, is necessary to limit the output currents. This work proposes a current reference generation called negative sequence minimization (NSM). With this method is possible to find the maximum reactive power references, in order to keep the output current limited. For instance, given an active power reference and a set of positive and negative sequence voltages, related to a generic unbalanced voltage dip, is possible to find the reactive power references without exceeding the maximum output converter output current. Another advantage of this strategy is that the grid voltage angles are not required to implement the algorithm.

Simulation and experimental results have shown the feasibility and the effectiveness of the proposed method.

Author details

Ivan Jorge Gabe [1*], Humberto Pinheiro[2] and Hilton Abílio Gründling[2]

*Address all correspondence to: ivangabe@gmail.com

1 Federal Institute of Rio Grande do Sul-IFRS, Farroupilha, Brazil

2 Federal University of Santa Maria, Santa Maria, Brazil

References

[1] Tsili, M, & Papathanassiou, S. A review of grid code technical requirements for wind farms. IET Renewable Power Generation (2009). , 3(3), 308-332.

[2] Alegría, I. M, Andreu, J, Martín, J L, Ibañez, P, Villate, J L, & Camblong, H. Connection requirements for wind farms: A survey on technical requirements and regulation. In ELSEVIER Renewable and Sustainable Energy Reviews, (2007). , 11(8), 1858-1872.

[3] Ministry for the EnvironmentNature Conservation and Nuclear Safety. "Ordinance on System Services by Wind Energy Plants" (System Service Ordinance-SDLWindV)". http://www.erneuerbareenergien.de/files/pdfs/allgemein/application/pdf/sdl_windv_en.pdf.accessed 3 July (2012).

[4] Bollen, M, & Zhang, J. L D. Different methods for classification of three-phase unbalanced voltage dips due to faults. In ELSEVIER Renewable and Sustainable Energy Reviews, (2003). , 11(1), 59-69.

[5] Bollen, M, & Zhang, J. L D. Characteristic of Voltage Dips (Sags) in Power Systems. IEEE Transactions on Power Delivery, (2000). , 13(2), 827-832.

[6] Gabe, I J, & Pinheiro, H. Impact of Unbalance Voltage Dips on the Behaviour of Voltage Source Inverters. In proceedings of Brazilian Power Electronics Conference (2009). COBEP'09, Sept. 27 2009-Oct. Bonito-MS Brazil., 1, 2009-956.

[7] Gabe, I J, Palha, F K, & Pinheiro, H. Grid Connected Voltage Source Inverter Control During Voltage Dips. In proceedings of IEEE Annual Conference 35th Industrial Electronics, (2009). IECON'Nov 2009, 4571- 4576., 09, 3-5.

[8] Teodorescu, R, Liserre, M, & Rodrígues, P. Grid Converters for Photovoltaic and Wind Power Systems. Wiley April (2011).

[9] Song, H S, & Nam, K. Dual Current Control Scheme for PWM Converter under Unbalanced Input Voltage Conditions. IEEE Transactions on Industrial Electronics (1999). , 46(5), 953-959.

[10] Rioual, P, Pouliquen, H, & Louis, J. P. Regulation of a PWM Rectifier in the Unbalanced Network State Using a Generalized Model. IEEE Transactions on Power Electronics (1996). , 11(3), 495-502.

[11] Wang, F, Duarte, J L, Hendrix, M, & Design, M. and Analysis of Active Power Control Strategies for Distributed Generation Inverters under Unbalanced Grid Faults. IET Generation, Transmission and Distribution (2010). , 4(8), 905-916.

[12] Rodriguez, P, Timbus, A. V, Teodeorescu, R, Liserre, M, & Blaabjerg, F. Independent PQ Control for Distributed Power Generation Systems under Grid Faults. In proceedings of 32° Annual IEEE Industrial Electronics Conference, IECON'06, (2006). Paris France.

[13] Lee, C T, Hsu, C H, & Cheng, P T. A Low-Voltage Ride-Through Technique for Grid-Connected Converters of Distributed Energy Resources. IEEE Transactions on Industry Application (2011). , 47(4), 1821-1832.

[14] Fischer, M, & Schellschmidt, M. Fault Ride Through performance of Wind Energy Converters with FACTS capabilities in response to up-to-date German grid connection requirements. In proceedings of European Wind Energy Conference and Exhibition, EWEC2010, (2010). Warsaw Poland.

[15] Brazilian National System Operator (ONS)Acompanhamento Mensal da Geração de Energia das Usinas Eolielétricas com Programação e Despacho Centralizados pela ONS (2012). http://www.ons.org.br/download/resultados_operacao/boletim_mensal_geracao_eolica/Boletim_Eolica_fev-2012.pdf.acessed on 27 july 2012).

[16] Fortescue, C L. Method of symmetrical co-ordinates applied to the solution of polyphase networks. Transaction of the Electrical Engineers (1928). , 37-1027.

[17] Gabe, I J, Montagner, V F, & Pinheiro, H. Design and Implementation of a Robust Current Controller for VSI Connected to the Grid Through an LCL Filter. IEEE Transactions on Power Electronics (2009). , 24(6), 1444-1452.